12 AUG. 1948

NATIONAL ADVISORY COMMITTEE FOR AERONAUTICS

TECHNICAL NOTE

No. 1672

SUPERSONIC WAVE DRAG OF NONLIFTING SWEPTBACK

TAPERED WINGS WITH MACH LINES BEHIND

THE LINE OF MAXIMUM THICKNESS

By Kenneth Margolis

Langley Aeronautical Laboratory
Langley Field, Va.

Washington
August 1948

NATIONAL ADVISORY COMMITTEE FOR AERONAUTICS

TECHNICAL NOTE NO. 1672

SUPERSONIC WAVE DRAG OF NONLIFTING SWEPTBACK

TAPERED WINGS WITH MACH LINES BEHIND

THE LINE OF MAXIMUM THICKNESS

By Kenneth Margolis

SUMMARY

A theoretical investigation of the supersonic wave drag of nonlifting sweptback tapered wings having thin symmetrical double-wedge airfoil sections with maximum thickness at 50 percent chord has been presented in NACA TN No. 1448. The present paper extends the investigation to include "supersonic" maximum-thickness edges; that is, the flight velocity component normal to the line of maximum thickness is supersonic. This condition exists at Mach numbers for which the Mach lines have angles of sweep greater than that of the line of maximum thickness.

For wings of equal root bending stress (and hence of different aspect ratio) and given sweepback, taper increases the wing wave-drag coefficient at Mach numbers for which the maximum-thickness line is moderately supersonic and has negligible effect at higher Mach numbers. This trend is similar to that evidenced by the effect of high aspect ratio for given sweepback and taper ratio. Comparisons on the basis of constant aspect ratio for given sweepback, however, indicate a decrease of the drag coefficient with taper at Mach numbers corresponding to moderately supersonic maximum-thickness lines and a negligible effect due to taper at the higher Mach numbers. For given taper ratio and aspect ratio, increased sweepback increases the drag coefficient at Mach numbers for which the maximum-thickness line is supersonic.

INTRODUCTION

In reference 1, equations are derived and calculations are presented for the supersonic wave drag of sweptback tapered wings with thin symmetrical double-wedge sections with maximum thickness at 50 percent chord (that is, rhombic profiles) at zero lift. The range of Mach number considered in reference 1 is between 1.0 and the value corresponding to the condition where the Mach lines are parallel to the maximum-thickness line, that is, the Mach number range corresponding to "subsonic" maximum-thickness lines. (When the flight velocity component normal to an edge is subsonic, the edge is termed a "subsonic" edge.) This condition exists at Mach numbers for which the Mach lines have angles of sweep less than that of the line of maximum thickness.

The present paper completes the wave-drag investigation of nonlifting tapered wings by extending the Mach number range to include "supersonic" maximum-thickness lines; that is, the region where the Mach lines have angles of sweep greater than that of the line of maximum thickness.

Accordingly, equations are derived for the supersonic wave drag of
sweptback tapered wings with thin rhombic sections at zero lift. Calcu-
lations are presented for some representative plan forms. As in
reference 1, the airfoil sections and wing tips are chosen parallel to
the direction of flight, and the angle of sweepback is referred to that
of the line of maximum thickness. For purposes of completeness, the
results obtained in reference 1 for the lower supersonic Mach numbers are
included in the discussion and conclusions of the present investigation.

SYMBOLS

x, y, z Cartesian coordinates

V velocity in flight direction

ρ density of air

Δp pressure increment

q dynamic pressure $\left(\frac{1}{2}\rho V^2\right)$

φ disturbance-velocity potential

M Mach number

$\beta = \sqrt{M^2 - 1}$

dz/dx slope of airfoil surface, measured in flight direction

a root semichord, measured in flight direction

c chord length at spanwise station y, measured in flight direction

t maximum thickness of section at spanwise station y

Λ angle of sweep of maximum-thickness line, degrees

m_0 slope of line of maximum thickness $(\cot \Lambda)$

m_1 slope of wing leading edge

m_2 slope of wing trailing edge $\left(\frac{m_1 m_0}{2m_1 - m_0}\right)$

b span of wing

$d = \dfrac{b/2}{m_0}$

S   wing area

A   aspect ratio $\left(b^2/S\right)$

λ taper ratio (ratio of tip chord to root chord)

c_{d_∞} section wave-drag coefficient at spanwise station y
             exclusive of tip effect

$c_{d_{tip}}$ increment in section wave-drag coefficient at spanwise
             station y due to tip

c_d section wave-drag coefficient at spanwise station y
             $\left(c_{d_\infty} + c_{d_{tip}}\right)$

C_{D_∞} wing wave-drag coefficient exclusive of tip effect

$C_{D_{tip}}$ increment in wing wave-drag coefficient due to tip

C_D wing wave-drag coefficient $\left(C_{D_\infty} + C_{D_{tip}}\right)$

Subscript s refers to conditions at root

ANALYSIS

The analysis is essentially that used in references 1 and 2. A
brief outline of the basic equations is included for convenience.

The assumptions of small disturbances and a constancy of sonic
velocity throughout the fluid lead to the linearized equation for the
disturbance-velocity potential φ

$$\left(1 - M^2\right)\varphi_{xx} + \varphi_{yy} + \varphi_{zz} = 0 \qquad (1)$$

where M is the Mach number of the flow and the derivatives are taken
with respect to the variables x, y, and z of the Cartesian coordinate
system. On the basis of this linear theory a solution for a uniform
semi-infinite sweptback line of sources is derived in reference 2. The
pressure field associated with this solution corresponds to that over an
airfoil of wedge section. The pressure coefficient $\Delta p/q$ at a spanwise
station y and point x along the wedge is, for $\beta \leqq \dfrac{1}{m_1}$,

$$\frac{\Delta p}{q} = \frac{2}{\pi} \frac{dz}{dx} \frac{m_1}{\sqrt{1 - m_1^2 \beta^2}} \cosh^{-1} \frac{x - m_1 \beta^2 y}{\beta |y - m_1 x|} \qquad (2a)$$

and, for $\beta > \frac{1}{m_1}$,

$$\frac{\Delta p}{q} = \frac{2}{\pi} \frac{dz}{dx} \frac{m_1}{\sqrt{m_1^2 \beta^2 - 1}} \cos^{-1} \frac{x - m_1 \beta^2 y}{\beta |y - m_1 x|} \qquad (2b)$$

where m_1 is the slope of the leading edge of the wing, dz/dx is the tangent of the half-wedge angle (approx. equal to half-wedge angle since the angle is small), $\beta = \sqrt{M^2 - 1}$, and the origin of the line source is taken at $(0,0)$. In the region between the leading edge and the Mach cone $\left(\text{that is, } \frac{1}{\beta}x \leqq y \leqq m_1 x\right)$, the real part of $\cos^{-1} \frac{x - m_1 \beta^2 y}{\beta |y - m_1 x|}$ is constant and equal to π. Equation (2b) then reduces to

$$\frac{\Delta p}{q} = 2 \frac{dz}{dx} \frac{m_1}{\sqrt{m_1^2 \beta^2 - 1}} \qquad (2c)$$

The distribution of pressure over sweptback wings of desired plan form and profile is obtained by superposition of solutions for wedge-type airfoils. Reference 1 adequately describes the superpositions necessary to satisfy the boundary conditions over the surface of a tapered wing of rhombic section, and therefore the procedure will not be restated herein. Figure 1 shows the distributions of sinks and sources for a tapered wing and identifies the system of axes and the symbols associated with the derivation of the drag equations.

The disturbances caused by the elementary line sources and sinks are limited to the regions enclosed by their Mach cones. Figure 2 shows the Mach line configuration for the tapered-wing plan forms and indicates the regions of the wing affected by each line source and sink. For purposes of simplification the tapered wings considered were restricted to those with no tip effects other than the effects each tip exerts on its own half of the wing. For a wing of taper ratio 0, no tip effects need be considered since the Mach lines originating at the tip do not enclose any part of the wing.

The pressure coefficients obtained from superposition of solutions given in equations (2) are converted into drag coefficients by the following relations:

$$C_D = \frac{2}{S} \int_0^{b/2} c_d c \; dy$$

$$= \frac{4}{S} \int_0^{b/2} \int_{L.E.}^{T.E.} \frac{\Delta p}{q} \frac{dz}{dx} \; dx \; dy \qquad (3)$$

where b is the wing span, S is the wing area, dz/dx is the slope of the airfoil surface, and L.E. and T.E. denote leading edge and trailing edge, respectively.

DERIVATION OF GENERALIZED EQUATIONS

By appropriate superposition of solutions for wedge-type airfoils, the pressure field is obtained for a tapered wing with leading edge, trailing edge, and line of maximum thickness sweptback. The drag equations are derived for half of the wing since the drag is distributed symmetrically over both halves. The induced effects of the opposite half-wing are represented by the conjugate terms in the integrands of the drag integrals.

For a rhombic profile,

$$\left|\frac{dz}{dx}\right| = \frac{t}{c}$$

where t/c is the section thickness ratio. The generalized equations for supersonic wave drag exclusive of tip effects are obtained as follows (see fig. 3 for information pertinent to integration limits):

For $\quad \dfrac{1}{m_0} \leqq \beta \leqq \dfrac{1}{m_1},$

$$\frac{\pi S C_{D_\infty}}{8(t/c)^2} = \frac{\pi}{4(t/c)^2} \int_0^{b/2} c_{d_\infty} c \, dy$$

$$= \frac{m_1}{\sqrt{1 - m_1{}^2 \beta^2}} \left(\int_0^{m_0 d} \int_{\frac{y - m_1 a}{m_1}}^{\frac{y}{m_0}} A \, dx \, dy - \int_0^{m_0 d} \int_{\frac{y}{m_0}}^{\frac{y + m_2 a}{m_2}} A \, dx \, dy \right)$$

$$+ \frac{2 m_0}{\sqrt{m_0{}^2 \beta^2 - 1}} \left(\int_0^{\frac{m_2 a}{m_2 \beta - 1}} \int_{\frac{y}{m_0}}^{y\beta} \pi \, dx \, dy + \int_{\frac{m_2 a}{m_2 \beta - 1}}^{m_0 d} \int_{\frac{y}{m_0}}^{\frac{y + m_2 a}{m_2}} \pi \, dx \, dy \right.$$

$$\left. + \int_0^{\frac{m_2 a}{m_2 \beta - 1}} \int_{y\beta}^{\frac{y + m_2 a}{m_2}} B \, dx \, dy \right) \tag{4a}$$

For $\beta > \dfrac{1}{m_1}$,

$$\frac{\pi S C_{D_\infty}}{8(t/c)^2} = \frac{\pi}{4(t/c)^2} \int_0^{b/2} c_{d_\infty} c \, dy$$

$$= \frac{m_1}{\sqrt{m_1{}^2\beta^2 - 1}} \left(\int_0^{\frac{m_0 a}{m_0\beta-1}} \int_{\frac{y-m_1 a}{m_1}}^{y\beta-a} \pi \, dx \, dy - \int_{\frac{m_0 a}{m_0\beta-1}}^{\frac{2m_2 a}{m_2\beta-1}} \int_{\frac{y}{m_0}}^{y\beta-a} \pi \, dx \, dy \right.$$

$$- \int_{\frac{2m_2 a}{m_2\beta-1}}^{m_0 d} \int_{\frac{y}{m_0}}^{\frac{y+m_2 a}{m_2}} \pi \, dx \, dy + \int_{\frac{m_0 a}{m_0\beta-1}}^{m_0 d} \int_{\frac{y-m_1 a}{m_1}}^{\frac{y}{m_0}} \pi \, dx \, dy$$

$$+ \int_0^{\frac{m_0 a}{m_0\beta-1}} \int_{y\beta-a}^{\frac{y}{m_0}} C \, dx \, dy - \int_0^{\frac{m_0 a}{m_0\beta-1}} \int_{\frac{y}{m_0}}^{\frac{y+m_2 a}{m_2}} C \, dx \, dy$$

$$\left. - \int_{\frac{m_0 a}{m_0\beta-1}}^{\frac{2m_2 a}{m_2\beta-1}} \int_{y\beta-a}^{\frac{y+m_2 a}{m_2}} C \, dx \, dy \right) + \frac{2m_0}{\sqrt{m_0{}^2\beta^2 - 1}} \left(\int_0^{\frac{m_2 a}{m_2\beta-1}} \int_{\frac{y}{m_0}}^{y\beta} \pi \, dx \, dy \right.$$

$$\left. + \int_{\frac{m_2 a}{m_2\beta-1}}^{m_0 d} \int_{\frac{y}{m_0}}^{\frac{y+m_2 a}{m_2}} \pi \, dx \, dy + \int_0^{\frac{m_2 a}{m_2\beta-1}} \int_{y\beta}^{\frac{y+m_2 a}{m_2}} B \, dx \, dy \right) \qquad (4b)$$

where

$$A = \cosh^{-1}\frac{x + a + m_1\beta^2 y}{\beta\,|y + m_1(x + a)|} + \cosh^{-1}\frac{x + a - m_1\beta^2 y}{\beta\,|y - m_1(x + a)|}$$

$$B = \cos^{-1}\frac{x + m_0\beta^2 y}{\beta\,|y + m_0 x|} + \cos^{-1}\frac{x - m_0\beta^2 y}{\beta\,|y - m_0 x|}$$

and

$$C = \cos^{-1}\frac{x + a + m_1\beta^2 y}{\beta\,|y + m_1(x + a)|} + \cos^{-1}\frac{x + a - m_1\beta^2 y}{\beta\,|y - m_1(x + a)|}$$

It should be noted that equations (4) give the drag for plan-form configurations where the tip is placed farther spanwise than the points of intersection between the Mach lines and the trailing edge. (See fig. 3.) Deletion of certain integrals and appropriate changes in the y limits of other integrals may be made for configurations where the tip is placed nearer the root chord. These equations are evaluated and the resulting section wave-drag and wing wave-drag formulas for all tapered plan forms are presented in appendix A.

As stated previously, the tapered wings considered have no tip effects other than those that each tip exerts on its own half of the wing; that is, the Mach lines from one tip do not enclose any part of the opposite half-wing. This condition is expressed mathematically as follows:

$$\text{Aspect ratio} = \frac{2 d m_0}{a(1 + \lambda)} \geqq \frac{4 m_1}{(1 + \lambda)(1 + m_1\beta)} \tag{5}$$

where λ is the taper ratio $\left(\dfrac{\text{Tip chord}}{\text{Root chord}}\right)$. It can be seen from equation (5) that this simplification does not materially limit the range of Mach number that may be considered. In fact, since these equations involve only Mach numbers corresponding to supersonic maximum-thickness lines, the limiting effect imposed in equation (5) is found to be negligible.

The wave-drag contribution of the tip is (fig. 3):

For $\dfrac{1}{m_0} \leqq \beta \leqq \dfrac{1}{m_1}$,

$$\frac{\pi S C_{D_{tip}}}{8(t/c)^2} = \frac{\pi}{4(t/c)^2} \int_{\frac{m_0 m_2 d(1+m_1\beta)-2m_1 m_2 a}{m_1(1+m_2\beta)}}^{m_0 d} c_{d_{tip}} c\ dy$$

$$= \frac{m_1}{\sqrt{1-m_1^2\beta^2}} \left[-\int_{\frac{m_0^2 d(1+m_1\beta)-m_1 m_0 a}{m_1(1+m_0\beta)}}^{m_0 d} \int_{\frac{m_0 d(1+m_1\beta)-m_1(a+\beta y)}{m_1}}^{\frac{y}{m_0}} D\ dx\ dy \right.$$

$$+ \int_{\frac{m_0^2 d(1+m_1\beta)-m_1 m_0 a}{m_1(1+m_0\beta)}}^{m_0 d} \int_{\frac{y}{m_0}}^{\frac{y+m_2 a}{m_2}} D\ dx\ dy$$

$$+ \left. \int_{\frac{m_0 m_2 d(1+m_1\beta)-2m_1 m_2 a}{m_1(1+m_2\beta)}}^{\frac{m_0^2 d(1+m_1\beta)-m_1 m_0 a}{m_1(1+m_0\beta)}} \int_{\frac{m_0 d(1+m_1\beta)-m_1(a+\beta y)}{m_1}}^{\frac{y+m_2 a}{m_2}} D\ dx\ dy \right]$$

$$- \frac{2m_0}{\sqrt{m_0^2\beta^2-1}} \int_{\frac{m_2 d(1+m_0\beta)-m_2 a}{1+m_2\beta}}^{m_0 d} \int_{d(1+m_0\beta)-\beta y}^{\frac{y+m_2 a}{m_2}} E\ dx\ dy \qquad (6)$$

where

$$D = \cosh^{-1} \frac{m_1(x + a) - m_0 d - m_1{}^2\beta^2(y - m_0 d)}{m_1\beta \left| y - m_1(x + a) \right|}$$

and

$$E = \cos^{-1} \frac{x - d - m_0\beta^2(y - m_0 d)}{\beta \left| y - m_0 x \right|}$$

For $\beta > \dfrac{1}{m_1}$, equation (6) is still valid if $\sqrt{1 - m_1{}^2\beta^2}$ is changed to

$\sqrt{m_1{}^2\beta^2 - 1}$ and the inverse hyperbolic function $\cosh^{-1}$ is changed to

the inverse cosine function $\cos^{-1}$.

Equation (6) was solved for section wave drag and wing wave drag, and the results are presented in appendix B. The total wave-drag coefficients are then obtained by the following relations:

$$\left.\begin{aligned} c_d &= c_{d_\infty} + c_{d_{tip}} \\ C_D &= C_{D_\infty} + C_{D_{tip}} \end{aligned}\right\} \tag{7}$$

The value of $C_{D_{tip}}$ is found to be identically equal to zero for all cases satisfying the limitations imposed in equation (5) and, hence, $C_D = C_{D_\infty}$ for the tapered wings considered.

RESULTS AND DISCUSSION

The formulas presented in the appendixes apply to all conventional taper ratios $(0 \leq \lambda \leq 1)$. For the particular case of taper ratio 1 (untapered plan form) the equations presented in appendix A of reference 3

are in a more convenient form for calculation purposes. Calculations presented for wings with subsonic maximum-thickness lines are based on the formulas of reference 1.

Calculations are made for some typical tapered plan forms and also for a family of tapered wings considered in reference 1; members of a family are characterized by constant sweepback of the line of maximum thickness and a constant value of the parameter "moment of wing area about the root chord divided by the product of the root chord and the square of the root thickness." This area-moment condition is intended to imply that, to a first approximation, the root bending stress is the same for all members of any family having the same thickness ratio. (See fig. 5 of reference 1 for further details.)

Section wave drag.— Spanwise distributions of section wave drag for wings of taper ratio 0, 0.5, and 1.0 are presented in figure 4 for a Mach number of 3, aspect ratio 2, and sweepback of 60°. These representative spanwise drag distributions for wings with supersonic maximum-thickness lines differ markedly from those obtained at lower speeds where the wing is swept well behind the Mach lines. All sections have positive drag at speeds corresponding to supersonic maximum-thickness lines, whereas, at the lower Mach numbers, outboard sections experience negative drag. (See figs. 6 to 10 of reference 1.)

Wing wave drag.— Variations of wing wave-drag coefficient with Mach number for constant-aspect-ratio wings of taper ratios 0 and 1.0 and 60° sweepback are presented in figures 5(a) and 5(b) for aspect ratios 2 and 3, respectively. For wings of constant aspect ratio, taper increases the drag coefficient at Mach numbers for which the maximum-thickness line is substantially subsonic, decreases the drag coefficient in the intermediate range, and has negligible effect when the maximum-thickness line is highly supersonic. For comparison purposes, the result for the straight wing of infinite aspect ratio (two-dimensional case) is included in figures 5 to 7. A typical variation in wing wave-drag coefficient with Mach number is shown in figure 6 for wings of equal root bending stress. (The data for the curves between Mach numbers 1 and 2 are taken from fig. 12 of reference 1.) Taper is shown to reduce the wing wave-drag coefficient at Mach numbers for which the maximum-thickness line is substantially subsonic, increase the drag coefficient in the intermediate range, and have little effect when the maximum-thickness line is highly supersonic. These trends are similar to the ones shown by the effect of high aspect ratio on the wave-drag coefficient of wings for a given taper ratio. (See fig. 7.) It must be remembered, however, that for the wings of equal root bending stress, those with greater taper have higher aspect ratios, and hence the drag behavior of these wings is, in effect, due to aspect-ratio variations.

Variation of wing wave-drag coefficient with sweepback for taper ratio 0.5 and aspect ratio 2 at a Mach number of 3 (supersonic maximum-thickness line) is shown in figure 8. Increased sweepback increases the drag rather than decreases the drag as is the case at lower Mach numbers, that is, for subsonic maximum-thickness lines. Calculations at other

Mach numbers show similar results for the effect of sweepback. It should be borne in mind, however, that a constant aspect ratio was maintained; that is, increased sweepback was obtained by sliding each section rearward rather than rotating the wing panels rearward.

CONCLUSIONS

The theoretical investigation of supersonic wave drag of sweptback tapered wings at zero lift with thin symmetrical double-wedge sections with maximum thickness at 50 percent chord (rhombic profiles) has been extended to include "supersonic" maximum-thickness lines; that is, the flight velocity component normal to the line of maximum thickness is supersonic. This condition exists at Mach numbers for which the Mach lines have angles of sweep greater than that of the line of maximum thickness. For purposes of completeness, the results obtained in NACA TN No. 1448 for "subsonic" maximum-thickness lines are included in the following conclusions.

1. For wings of constant aspect ratio and given sweepback, taper increases the wing wave-drag coefficient at Mach numbers for which the maximum-thickness line is substantially subsonic, decreases the drag coefficient in the near-sonic through moderately supersonic range, and has negligible effect when the maximum-thickness line is highly supersonic.

2. For given sweep and taper ratio, higher aspect ratios reduce the wing wave-drag coefficient at Mach numbers for which the line of maximum thickness is substantially subsonic, increase the drag coefficient in the intermediate range, and have negligible effect when the maximum-thickness line is highly supersonic.

3. For wings of equal root bending stress and given sweepback, taper reduces the wing wave-drag coefficient at Mach numbers for which the maximum-thickness line is substantially subsonic, increases the drag coefficient in the intermediate range, and has negligible effect when the maximum-thickness line is highly supersonic.

4. For given taper ratio and aspect ratio, increased sweepback reduces the wing wave-drag coefficient at speeds corresponding to subsonic maximum-thickness lines and increases the drag coefficient when the maximum-thickness line is supersonic.

Langley Aeronautical Laboratory
    National Advisory Committee for Aeronautics
        Langley Field, Va., February 25, 1948

<center>APPENDIX A</center>

<center>EVALUATION OF EQUATIONS (4) FOR SECTION WAVE</center>

<center>DRAG AND WING DRAG EXCLUSIVE OF</center>

<center>TIP EFFECTS $\left(\beta \geqq \dfrac{1}{m_0}; \ 0 \leqq \lambda \leqq 1\right)$</center>

<center>Section Drag</center>

For $\dfrac{1}{m_0} \leqq \beta \leqq \dfrac{1}{m_1}$,

$$\frac{\pi c_{d_\infty} c}{4(t/c)^2} = A + B \qquad\qquad \text{for} \qquad 0 \leqq y \leqq \frac{am_2}{\beta m_2 - 1}$$

$$= A + C \qquad\qquad\qquad\qquad \frac{am_2}{\beta m_2 - 1} < y \leqq m_0 d$$

where

$$A = \frac{m_1}{\sqrt{1 - \beta^2 m_1^2}} \left[2\, \frac{y(m_0 + m_1) + am_0 m_1}{m_0 m_1} \cosh^{-1} \frac{y(1 + m_1 m_0 \beta^2) + am_0}{\beta\left| y(m_0 + m_1) + am_1 m_0 \right|} \right.$$

$$- 2\, \frac{y(m_0 - m_1) - am_0 m_1}{m_0 m_1} \cosh^{-1} \frac{y(1 - m_0 m_1 \beta^2) + am_0}{\beta\left| y(m_0 - m_1) - am_0 m_1 \right|} - \frac{2y}{m_1} \cosh^{-1} \frac{1 + m_1^2 \beta^2}{2m_1 \beta}$$

$$- \frac{y(m_1 + m_2) + 2am_1 m_2}{m_1 m_2} \cosh^{-1} \frac{y(1 + m_1 m_2 \beta^2) + 2am_2}{\beta\left| y(m_1 + m_2) + 2am_1 m_2 \right|}$$

$$+ \frac{y(m_2 - m_1) - 2am_1 m_2}{m_1 m_2} \cosh^{-1} \frac{y(1 - m_1 m_2 \beta^2) + 2am_2}{\beta\left| y(m_2 - m_1) - 2am_1 m_2 \right|} \right]$$

$$B = \frac{2m_0}{\sqrt{\beta^2 m_0{}^2 - 1}} \left[\frac{y\left(m_0 + m_2\right) + am_0m_2}{m_0m_2} \cos^{-1} \frac{y\left(1 + m_0m_2\beta^2\right) + am_2}{\beta \left| y\left(m_0 + m_2\right) + am_0m_2 \right|} \right.$$

$$\left. - \frac{y\left(m_2 - m_0\right) - am_0m_2}{m_0m_2} \cos^{-1} \frac{y\left(1 - m_0m_2\beta^2\right) - am_2}{\beta \left| y\left(m_2 - m_0\right) - am_0m_2 \right|} \right]$$

and

$$C = \frac{2m_0\pi}{\sqrt{\beta^2 m_0{}^2 - 1}} \left(\frac{y + am_2}{m_2} - \frac{y}{m_0} \right)$$

For $\beta > \dfrac{1}{m_1}$,

$$\frac{\pi c_{d_\infty} c}{4\left(t/c\right)^2} = A + B + C \qquad\qquad \text{for} \qquad 0 \leqq y \leqq \frac{am_2}{\beta m_2 - 1}$$

$$= B + C + D \qquad\qquad \frac{am_2}{\beta m_2 - 1} < y \leqq \frac{am_0}{\beta m_0 - 1}$$

$$= C + D + E \qquad\qquad \frac{am_0}{\beta m_0 - 1} < y \leqq \frac{2am_2}{\beta m_2 - 1}$$

$$= D \qquad\qquad\qquad\qquad \frac{2am_2}{\beta m_2 - 1} < y \leqq m_0 d$$

where

$$A = \frac{2m_0}{\sqrt{\beta^2 m_0{}^2 - 1}} \left[\frac{y(m_0 + m_2) + am_0 m_2}{m_0 m_2} \cos^{-1} \frac{y(1 + m_0 m_2 \beta^2) + am_2}{\beta \left| y(m_0 + m_2) + am_0 m_2 \right|} \right.$$

$$\left. + \frac{y(m_0 - m_2) + am_0 m_2}{m_0 m_2} \cos^{-1} \frac{y(1 - m_0 m_2 \beta^2) + am_2}{\beta \left| y(m_2 - m_0) - am_0 m_2 \right|} \right]$$

$$B = \frac{2m_1}{\sqrt{\beta^2 m_1{}^2 - 1}} \left[\frac{y(m_0 + m_1) + am_0 m_1}{m_0 m_1} \cos^{-1} \frac{y(1 + m_0 m_1 \beta^2) + am_0}{\beta \left| y(m_0 + m_1) + am_0 m_1 \right|} \right.$$

$$\left. + \frac{y(m_1 - m_0) + am_0 m_1}{m_0 m_1} \cos^{-1} \frac{y(1 - m_0 m_1 \beta^2) + am_0}{\beta \left| y(m_0 - m_1) - am_1 m_0 \right|} \right]$$

$$C = - \frac{m_1}{\sqrt{\beta^2 m_1{}^2 - 1}} \left[\frac{y(m_2 + m_1) + 2am_1 m_2}{m_1 m_2} \cos^{-1} \frac{y(1 + m_1 m_2 \beta^2) + 2am_2}{\beta \left| y(m_1 + m_2) + 2am_1 m_2 \right|} \right.$$

$$\left. + \frac{y(m_1 - m_2) + 2am_1 m_2}{m_1 m_2} \cos^{-1} \frac{y(1 - m_1 m_2 \beta^2) + 2am_2}{\beta \left| y(m_2 - m_1) - 2am_1 m_2 \right|} \right]$$

$$D = \frac{2m_0 \pi}{\sqrt{\beta^2 m_0{}^2 - 1}} \left(\frac{y + am_2}{m_2} - \frac{y}{m_0} \right)$$

and

$$E = \frac{2m_1 \pi}{\sqrt{\beta^2 m_1^2 - 1}} \left(\frac{y}{m_0} - \frac{y - am_1}{m_1} \right)$$

Wing Drag

For $\dfrac{1}{m_0} < \beta < \dfrac{1}{m_1}$,

$$\frac{\pi S C_{D_\infty}}{8(t/c)^2} = A + B \qquad\qquad\qquad \text{for} \quad m_0 d \leqq \frac{am_2}{\beta m_2 - 1}$$

$$\qquad\qquad\qquad = A + C \qquad\qquad\qquad m_0 d > \frac{am_2}{\beta m_2 - 1}$$

where

$$A = \frac{2a^2 m_0^3 m_1}{\left(m_0^2 - m_1^2\right)\sqrt{\beta^2 m_0^2 - 1}} \; \cos^{-1} \frac{a - d\left(\beta^2 m_0^2 - 1\right)}{am_0 \beta}$$

$$+ \frac{m_0 \left[(m_0 + m_1)d + am_1 \right]^2}{(m_0 + m_1)\sqrt{1 - \beta^2 m_1^2}} \; \cosh^{-1} \frac{\left(1 + m_0 m_1 \beta^2\right)d + a}{\beta \left| (m_0 + m_1)d + am_1 \right|}$$

$$- \frac{m_0 \left[(m_0 - m_1)d - am_1 \right]^2}{(m_0 - m_1)\sqrt{1 - \beta^2 m_1^2}} \; \cosh^{-1} \frac{\left(1 - m_0 m_1 \beta^2\right)d + a}{\beta \left| (m_0 - m_1)d - am_1 \right|}$$

$$+ \frac{a^2 m_1 m_0{}^2}{\left(m_0 + m_1\right)\sqrt{1 - \beta^2 m_1{}^2}} \cosh^{-1} \frac{1}{m_1 \beta}$$

$$- \frac{4a^2 m_1 m_2{}^3}{\left(m_2{}^2 - m_1{}^2\right)\sqrt{\beta^2 m_2{}^2 - 1}} \cos^{-1} \frac{2am_2 - dm_0\left(\beta^2 m_2{}^2 - 1\right)}{2am_2{}^2 \beta}$$

$$- \frac{d^2 m_0{}^2}{\sqrt{1 - \beta^2 m_1{}^2}} \cosh^{-1} \frac{1 + \beta^2 m_1{}^2}{2m_1 \beta}$$

$$- \frac{\left[\left(m_2 + m_1\right)dm_0 + 2am_1 m_2\right]^2}{2m_2\left(m_1 + m_2\right)\sqrt{1 - \beta^2 m_1{}^2}} \cosh^{-1} \frac{\left(1 + m_1 m_2 \beta^2\right)dm_0 + 2am_2}{\beta \left|\left(m_1 + m_2\right)dm_0 + 2am_1 m_2\right|}$$

$$+ \frac{\left[\left(m_2 - m_1\right)dm_0 - 2am_1 m_2\right]^2}{2m_2\left(m_2 - m_1\right)\sqrt{1 - \beta^2 m_1{}^2}} \cosh^{-1} \frac{\left(1 - m_1 m_2 \beta^2\right)dm_0 + 2am_2}{\beta \left|\left(m_2 - m_1\right)dm_0 - 2am_1 m_2\right|}$$

$$B = \frac{2a^2 m_0 m_2{}^3}{\left(m_2{}^2 - m_0{}^2\right)\sqrt{\beta^2 m_2{}^2 - 1}} \cos^{-1} \frac{am_2 - dm_0\left(\beta^2 m_2{}^2 - 1\right)}{am_2{}^2 \beta}$$

$$+ \frac{\left[\left(m_2 + m_0\right)dm_0 + am_2 m_0\right]^2}{m_2\left(m_2 + m_0\right)\sqrt{\beta^2 m_0{}^2 - 1}} \cos^{-1} \frac{\left(1 + m_2 m_0 \beta^2\right)dm_0 + am_2}{\beta\left|\left(m_2 + m_0\right)dm_0 + am_2 m_0\right|}$$

$$- \frac{\left[\left(m_2 - m_0\right)dm_0 - am_2 m_0\right]^2}{m_2\left(m_2 - m_0\right)\sqrt{\beta^2 m_0{}^2 - 1}} \cos^{-1} \frac{\left(1 - m_2 m_0 \beta^2\right)dm_0 + am_2}{\beta\left|\left(m_2 - m_0\right)dm_0 - am_2 m_0\right|}$$

$$- \frac{4a^2 m_0{}^2 m_1{}^2}{\left(m_0 + m_1\right)\left(3m_1 - m_0\right)\sqrt{\beta^2 m_0{}^2 - 1}} \cos^{-1} \frac{1}{m_0 \beta}$$

$$+ \frac{a^2 m_2 m_0{}^2}{\left(m_2 + m_0\right)\sqrt{\beta^2 m_2{}^2 - 1}} \cos^{-1} \frac{1}{m_2 \beta}$$

and

$$C = \frac{a^2 m_2 m_0{}^2}{\left(m_2 + m_0\right)\sqrt{\beta^2 m_2{}^2 - 1}} \cos^{-1} \frac{1}{m_2 \beta}$$

$$- \frac{4a^2 m_0{}^2 m_1{}^2}{\left(m_0 + m_1\right)\left(3m_1 - m_0\right)\sqrt{\beta^2 m_0{}^2 - 1}} \cos^{-1} \frac{1}{m_0 \beta}$$

$$+ \frac{2a^2 m_2{}^3 m_0 \pi}{\left(m_2{}^2 - m_0{}^2\right)\sqrt{\beta^2 m_2{}^2 - 1}}$$

$$+ \frac{m_0 \pi}{\sqrt{\beta^2 m_0{}^2 - 1}} \left[\frac{dm_0\left(dm_0 - dm_2 + 2am_2\right)}{m_2} - \frac{a^2 m_0 m_2}{m_2 - m_0}\right]$$

For $\beta = \dfrac{1}{m_1}$ and $m_0 d \lessgtr \dfrac{am_2}{\beta m_2 - 1}$,

$$\frac{\pi S C_{D_\infty}}{8(t/c)^2} = \frac{2a^2 m_0{}^3 m_1}{\left(m_0{}^2 - m_1{}^2\right)\sqrt{\beta^2 m_0{}^2 - 1}}\cos^{-1}\frac{a - d\left(\beta^2 m_0{}^2 - 1\right)}{am_0\beta}$$

$$- \frac{4a^2 m_1 m_2{}^3}{\left(m_2{}^2 - m_1{}^2\right)\sqrt{\beta^2 m_2{}^2 - 1}}\cos^{-1}\frac{2am_2 - dm_0\left(\beta^2 m_2{}^2 - 1\right)}{2am_2{}^2\beta}$$

$$+ \frac{2a^2 m_0 m_2{}^3}{\left(m_2{}^2 - m_0{}^2\right)\sqrt{\beta^2 m_2{}^2 - 1}}\cos^{-1}\frac{am_2 - dm_0\left(\beta^2 m_2{}^2 - 1\right)}{am_2{}^2\beta}$$

$$+ \frac{\left[\left(m_2 + m_0\right)dm_0 + am_2 m_0\right]^2}{m_2\left(m_2 + m_0\right)\sqrt{\beta^2 m_0{}^2 - 1}}\cos^{-1}\frac{\left(1 + m_2 m_0\beta^2\right)dm_0 + am_2}{\beta\left|\left(m_2 + m_0\right)dm_0 + am_2 m_0\right|}$$

$$- \frac{\left[\left(m_2 - m_0\right)dm_0 - am_2 m_0\right]^2}{m_2\left(m_2 - m_0\right)\sqrt{\beta^2 m_0{}^2 - 1}}\cos^{-1}\frac{\left(1 - m_0 m_2\beta^2\right)dm_0 + am_2}{\beta\left|\left(m_2 - m_0\right)dm_0 - am_2 m_0\right|}$$

$$- \frac{4a^2 m_0{}^2 m_1{}^2}{\left(m_0 + m_1\right)\left(3m_1 - m_0\right)\sqrt{\beta^2 m_0{}^2 - 1}}\cos^{-1}\frac{1}{m_0\beta}$$

$$+ \frac{a^2 m_2 m_0{}^2}{\left(m_2 + m_0\right)\sqrt{\beta^2 m_2{}^2 - 1}}\cos^{-1}\frac{1}{m_2\beta} + \frac{a^2 m_1 m_0{}^2}{\left(m_0 + m_1\right)}$$

$$+ \frac{2m_0\left[\left(m_0{}^2 - m_1{}^2\right)d - am_1{}^2\right]\sqrt{m_1{}^2\left(a + d\right)^2 - d^2 m_0{}^2}}{m_0{}^2 - m_1{}^2}$$

$$+ \frac{\left[2am_2 m_1{}^2 - \left(m_2{}^2 - m_1{}^2\right)dm_0\right]\sqrt{d^2 m_0{}^2\left(m_1{}^2 - m_2{}^2\right) + 4am_2 m_1{}^2\left(am_2 + dm_0\right)}}{m_2\left(m_2{}^2 - m_1{}^2\right)}$$

For $\beta = \dfrac{1}{m_1}$ and $m_0 d > \dfrac{am_2}{\beta m_2 - 1}$,

$$\frac{\pi S C_{D_\infty}}{8(t/c)^2} = \frac{2a^2 m_0^3 m_1}{\left(m_0^2 - m_1^2\right)\sqrt{\beta^2 m_0^2 - 1}} \cos^{-1} \frac{a - d\left(\beta^2 m_0^2 - 1\right)}{am_0 \beta}$$

$$- \frac{4a^2 m_1 m_2^3}{\left(m_2^2 - m_1^2\right)\sqrt{\beta^2 m_2^2 - 1}} \cos^{-1} \frac{2am_2 - dm_0\left(\beta^2 m_2^2 - 1\right)}{2am_2^2 \beta}$$

$$- \frac{4a^2 m_0^2 m_1^2}{\left(m_0 + m_1\right)\left(3m_1 - m_0\right)\sqrt{\beta^2 m_0^2 - 1}} \cos^{-1} \frac{1}{m_0 \beta}$$

$$+ \frac{a^2 m_2 m_0^2}{\left(m_2 + m_0\right)\sqrt{\beta^2 m_2^2 - 1}} \cos^{-1} \frac{1}{m_2 \beta} + \frac{2a^2 m_2^3 m_0 \pi}{\left(m_2^2 - m_0^2\right)\sqrt{\beta^2 m_2^2 - 1}}$$

$$+ \frac{a^2 m_1 m_0^2}{\left(m_0 + m_1\right)} + \frac{m_0 \pi}{\sqrt{\beta^2 m_0^2 - 1}}\left[\frac{dm_0\left(dm_0 - dm_2 + 2am_2\right)}{m_2} - \frac{a^2 m_0 m_2}{m_2 - m_0}\right]$$

$$+ \frac{2m_0 \left[\left(m_0^2 - m_1^2\right)d - am_1^2\right]\sqrt{m_1^2(a + d)^2 - d^2 m_0^2}}{m_0^2 - m_1^2}$$

$$+ \frac{\left[2am_2 m_1^2 - \left(m_2^2 - m_1^2\right)dm_0\right]\sqrt{d^2 m_0^2\left(m_1^2 - m_2^2\right) + 4am_2 m_1^2\left(am_2 + dm_0\right)}}{m_2\left(m_2^2 - m_1^2\right)}$$

For $\quad \beta = \dfrac{1}{m_0},$

$$\frac{\pi S C_{D_\infty}}{8(t/c)^2} = \frac{m_0 \left[(m_0 + m_1)d + am_1\right]^2}{(m_0 + m_1)\sqrt{1 - \beta^2 m_1^2}} \cosh^{-1} \frac{\left(1 + m_0 m_1 \beta^2\right)d + a}{\beta \left|(m_0 + m_1)d + am_1\right|}$$

$$- \frac{m_0 \left[(m_0 - m_1)d - am_1\right]^2}{(m_0 - m_1)\sqrt{1 - \beta^2 m_1^2}} \cosh^{-1} \frac{\left(1 - m_0 m_1 \beta^2\right)d + a}{\beta \left|(m_0 - m_1)d - am_1\right|}$$

$$+ \frac{a^2 m_1 m_0^2}{(m_0 + m_1)\sqrt{1 - \beta^2 m_1^2}} \cosh^{-1} \frac{1}{m_1 \beta}$$

$$- \frac{4a^2 m_1 m_2^3}{(m_2^2 - m_1^2)\sqrt{\beta^2 m_2^2 - 1}} \cos^{-1} \frac{2am_2 - dm_0\left(\beta^2 m_2^2 - 1\right)}{2am_2^2 \beta}$$

$$- \frac{\left[(m_2 + m_1)dm_0 + 2am_1 m_2\right]^2}{2m_2(m_1 + m_2)\sqrt{1 - \beta^2 m_1^2}} \cosh^{-1} \frac{\left(1 + m_1 m_2 \beta^2\right)dm_0 + 2am_2}{\beta \left|(m_2 + m_1)dm_0 + 2am_1 m_2\right|}$$

$$+ \frac{\left[(m_2 - m_1)dm_0 - 2am_1 m_2\right]^2}{2m_2(m_2 - m_1)\sqrt{1 - \beta^2 m_1^2}} \cosh^{-1} \frac{\left(1 - m_1 m_2 \beta^2\right)dm_0 + 2am_2}{\beta \left|(m_2 - m_1)dm_0 - 2am_1 m_2\right|}$$

$$- \frac{d^2 m_0^2}{\sqrt{1 - \beta^2 m_1^2}} \cosh^{-1} \frac{1 + \beta^2 m_1^2}{2\beta m_1}$$

$$+ \frac{2a^2 m_0 m_2^3}{(m_2^2 - m_0^2)\sqrt{\beta^2 m_2^2 - 1}} \cos^{-1} \frac{am_2 - dm_0\left(\beta^2 m_2^2 - 1\right)}{am_2^2 \beta}$$

$$+ \frac{a^2 m_2 m_0^2}{(m_2 + m_0)\sqrt{\beta^2 m_2^2 - 1}} \cos^{-1} \frac{1}{m_2 \beta}$$

$$+ \frac{2a m_0^3 m_1 \sqrt{a(2d + e)}}{m_0^2 - m_1^2} - \frac{4a^2 m_0^2 m_1^2}{(m_0 + m_1)(3m_1 - m_0)}$$

$$+ \frac{2m_0^2 \left[(m_2^2 - m_0^2)d - a m_0 m_2\right] \sqrt{a m_2 (a m_2 + 2 m_0 d) - d^2 (m_2^2 - m_0^2)}}{m_2 (m_2^2 - m_0^2)}$$

For $\beta > \dfrac{1}{m_1}$,

$$\frac{\pi S C_{D_\infty}}{8(t/c)^2} = A + B + C \qquad \text{for} \qquad 0 \leqq m_0 d \leqq \frac{a m_2}{\beta m_2 - 1}$$

$$= B + C + D \qquad\qquad \frac{a m_2}{\beta m_2 - 1} < m_0 d \leqq \frac{a m_0}{\beta m_0 - 1}$$

$$= C + D + E \qquad\qquad \frac{a m_0}{\beta m_0 - 1} < m_0 d \leqq \frac{2 a m_2}{\beta m_2 - 1}$$

$$= F \qquad\qquad\qquad m_0 d > \frac{2 a m_2}{\beta m_2 - 1}$$

where

$$A = \frac{m_0^2\left[(m_2 + m_0)d + am_2\right]^2}{m_2(m_2 + m_0)\sqrt{\beta^2 m_0^2 - 1}} \cos^{-1} \frac{(1 + m_0 m_2 \beta^2)dm_0 + am_2}{\beta\left|(m_2 + m_0)dm_0 + am_2 m_0\right|}$$

$$- \frac{m_0^2\left[(m_2 - m_0)d - am_2\right]^2}{m_2(m_2 - m_0)\sqrt{\beta^2 m_0^2 - 1}} \cos^{-1} \frac{(1 - m_2 m_0 \beta^2)dm_0 + am_2}{\beta\left|(m_2 - m_0)dm_0 - am_0 m_2\right|}$$

$$+ \frac{2a^2 m_0 m_2^3}{(m_2^2 - m_0^2)\sqrt{\beta^2 m_2^2 - 1}} \cos^{-1} \frac{am_2 - dm_0(\beta^2 m_2^2 - 1)}{am_2^2 \beta}$$

$$B = \frac{2a^2 m_0^3 m_1}{(m_0^2 - m_1^2)\sqrt{\beta^2 m_0^2 - 1}} \cos^{-1} \frac{a - d(\beta^2 m_0^2 - 1)}{am_0 \beta}$$

$$+ \frac{m_0\left[(m_0 + m_1)d + am_1\right]^2}{(m_0 + m_1)\sqrt{\beta^2 m_1^2 - 1}} \cos^{-1} \frac{(1 + m_0 m_1 \beta^2)d + a}{\beta\left|(m_0 + m_1)d + am_1\right|}$$

$$- \frac{m_0\left[(m_0 - m_1)d - am_1\right]^2}{(m_0 - m_1)\sqrt{\beta^2 m_1^2 - 1}} \cos^{-1} \frac{(1 - m_0 m_1 \beta^2)d + a}{\beta\left|(m_0 - m_1)d - am_1\right|}$$

$$C = - \frac{4a^2 m_0^2 m_1^2}{(3m_1 - m_0)(m_1 + m_0)\sqrt{\beta^2 m_0^2 - 1}} \cos^{-1} \frac{1}{m_0 \beta}$$

$$+ \frac{\left[(m_2 - m_1)dm_0 - 2am_1 m_2\right]^2}{2m_2(m_2 - m_1)\sqrt{\beta^2 m_1^2 - 1}} \cos^{-1} \frac{\left(1 - m_1 m_2 \beta^2\right)dm_0 + 2am_2}{\beta \left| (m_2 - m_1)dm_0 - 2am_1 m_2 \right|}$$

$$- \frac{\left[(m_2 + m_1)dm_0 + 2am_1 m_2\right]^2}{2m_2(m_2 + m_1)\sqrt{\beta^2 m_1^2 - 1}} \cos^{-1} \frac{\left(1 + m_1 m_2 \beta^2\right)dm_0 + 2am_2}{\beta \left| (m_1 + m_2)dm_0 + 2am_1 m_2 \right|}$$

$$+ \frac{a^2 m_0^2 m_1}{(m_0 + m_1)\sqrt{\beta^2 m_1^2 - 1}} \cos^{-1} \frac{1}{m_1 \beta} + \frac{a^2 m_2 m_0^2}{(m_0 + m_2)\sqrt{\beta^2 m_2^2 - 1}} \cos^{-1} \frac{1}{m_2 \beta}$$

$$- \frac{4a^2 m_2^3 m_1}{(m_2^2 - m_1^2)\sqrt{\beta^2 m_2^2 - 1}} \cos^{-1} \frac{2am_2 - dm_0 \left(\beta^2 m_2^2 - 1\right)}{2am_2^2 \beta}$$

$$D = \frac{\pi m_0^2}{\sqrt{\beta^2 m_0^2 - 1}} \left[\frac{a^2 m_1}{m_1 - m_0} + \frac{d\left(dm_1 - dm_0 + 2am_1\right)}{m_1} \right]$$

$$+ \frac{2a^2 m_2^3 m_0 \pi}{(m_2^2 - m_0^2)\sqrt{\beta^2 m_2^2 - 1}}$$

$$E = \frac{\pi m_0}{\sqrt{\beta^2 m_1^2 - 1}} \left[- \frac{a^2 m_1^2}{m_0 - m_1} + d\left(dm_1 - dm_0 + 2am_1\right) \right] - \frac{2\pi a^2 m_1 m_0^3}{\sqrt{\beta^2 m_0^2 - 1}\left(m_1^2 - m_0^2\right)}$$

and

$$\frac{\pi}{\frac{1}{2}} \qquad a^2 m_2 \qquad b_2' \left(\frac{2am_2 + b_2'}{m_2}\right)$$

$$F = \frac{\pi m_0}{\sqrt{\beta^2 m_0^2 - 1}} \left[\frac{a^2 m_0 m_2}{3m_2 - m_0} + \frac{dm_0\left(2am_2 - dm_2 + dm_0\right)}{m_2} \right]$$

$$- \frac{a^2 m_1 m_0^2}{\left(3m_1 - m_0\right)\sqrt{\beta^2 m_2^2 - 1}} \cos^{-1} \frac{1}{\beta m_2} + \frac{a^2 m_1 m_0^2}{\left(m_0 + m_1\right)\sqrt{\beta^2 m_1^2 - 1}} \cos^{-1} \frac{1}{\beta m_1}$$

$$- \frac{4a^2 m_0^2 m_1^2}{\left(3m_1 - m_0\right)\left(m_0 + m_1\right)\sqrt{\beta^2 m_0^2 - 1}} \cos^{-1} \frac{1}{\beta m_0}$$

APPENDIX B

EVALUATION OF EQUATION (6) FOR TIP EFFECTS $\left(\beta \geqq \dfrac{1}{m_0}; \ 0 \leqq \lambda \leqq 1 \right)$

For aspect-ratio limitations, see equation (5).

Section Drag Increment-

For $\dfrac{1}{m_0} \leqq \beta \leqq \dfrac{1}{m_1}$,

$$\frac{\pi c_{d_{tip}} c}{4\left(t/c\right)^2} = A + B + C$$

where A is evaluated in the region $\dfrac{dm_0{}^2\left(1 + \beta m_1\right) - am_1 m_0}{m_1\left(1 + \beta m_0\right)} \leqq y \leqq dm_0$

and is equal to

$$\frac{2\left[y\left(m_0 - m_1\right) - am_1 m_0\right]}{m_0\sqrt{1 - m_1{}^2\beta^2}} \ \cosh^{-1} \frac{ym_1\left(1 - m_0 m_1 \beta^2\right) - dm_0{}^2\left(1 - m_1{}^2\beta^2\right) + am_1 m_0}{\beta m_1\left| y\left(m_0 - m_1\right) - am_0 m_1\right|}$$

$$- \ 2\left(y - dm_0\right) \cosh^{-1} \frac{ym_1 + am_1 m_0 - dm_0{}^2}{\beta m_1 m_0\left(dm_0 - y\right)}$$

B is evaluated in the region $\dfrac{dm_0 m_2\left(1 + \beta m_1\right) - 2am_1 m_2}{m_1\left(1 + \beta m_2\right)} \leqq y \leqq dm_0$

and is equal to

$$- \ \frac{2\left[\left(m_0 - m_1\right)y - am_0 m_1\right]}{m_0\sqrt{1 - m_1{}^2\beta^2}} \ \cosh^{-1} \frac{y\left(2m_1 - m_0 - m_1{}^2 m_0 \beta^2\right) + 2am_1 m_0 - dm_0{}^2\left(1 - m_1{}^2\beta^2\right)}{2\beta m_1\left| y\left(m_0 - m_1\right) - am_0 m_1\right|}$$

$$+ \ \left(y - dm_0\right) \cosh^{-1} \frac{y\left(2m_1 - m_0\right) + m_0\left(2am_1 - dm_0\right)}{\beta m_1 m_0\left(dm_0 - y\right)}$$

and C is evaluated in the region $\dfrac{dm_2\left(1 + \beta m_0\right) - am_2}{1 + \beta m_2} \leqq y \leqq dm_0$

and is equal to

$$\frac{2\left[y\left(m_2 - m_0\right) - am_2m_0\right]}{m_2\sqrt{\beta^2 m_0{}^2 - 1}} \cos^{-1} \frac{y\left(1 - m_0 m_2\beta^2\right) - dm_2\left(1 - m_0{}^2\beta^2\right) + am_2}{\beta\left|y\left(m_2 - m_0\right) - am_0m_2\right|}$$

$$- 2\left(y - dm_0\right)\cosh^{-1}\frac{y + m_2(a - d)}{\beta m_2\left(dm_0 - y\right)}$$

For $\beta > \dfrac{1}{m_1}$, use the same formulas as for $\dfrac{1}{m_0} \leqq \beta \leqq \dfrac{1}{m_1}$ but

change $\sqrt{1 - m_1{}^2\beta^2}$ to $\sqrt{\beta^2 m_1{}^2 - 1}$ and $\cosh^{-1}$ to $\cos^{-1}$ in the first term only of both A and B.

Wing Drag Increment

The increment in wing wave drag caused by the tip is identically equal to zero for all cases satisfying these aspect-ratio limitations.

REFERENCES

1. Margolis, Kenneth: Supersonic Wave Drag of Sweptback Tapered Wings
   at Zero Lift. NACA TN No. 1448, 1947.

2. Jones, Robert T.: Thin Oblique Airfoils at Supersonic Speed.
   NACA Rep. No. 851, 1946.

3. Margolis, Kenneth: Effect of Chordwise Location of Maximum Thickness
   on the Supersonic Wave Drag of Sweptback Wings. NACA TN No. 1543,
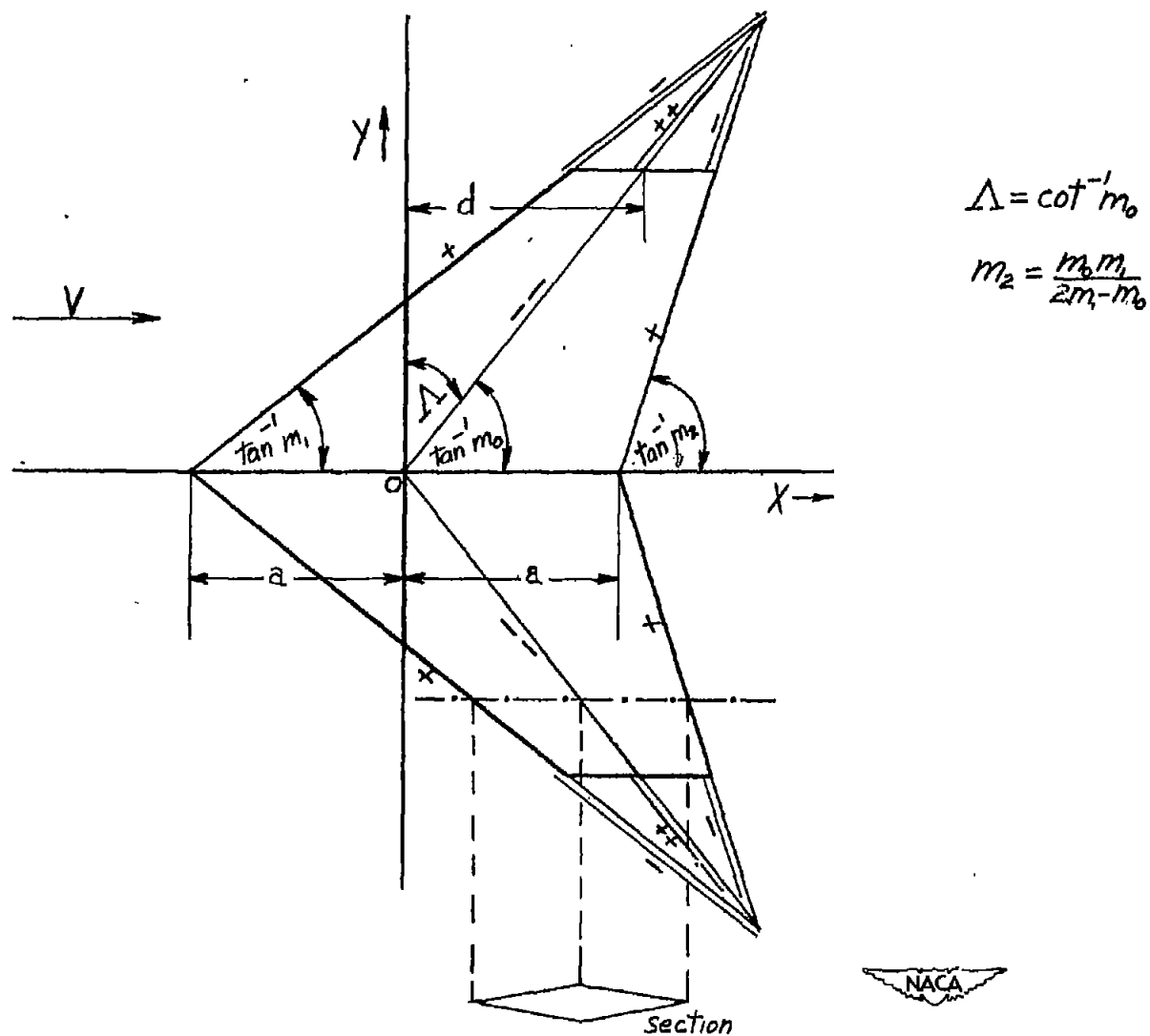   1948.

$$\Lambda = cot^{-1} m_0$$

$$m_2 = \frac{m_0 m_1}{2 m_1 - m_0}$$

Figure 1.- Symbols and distributions of sinks and sources for a tapered wing.

$$\frac{1}{m_0} < \beta < \frac{1}{m_1} \qquad\qquad \beta > \frac{1}{m_1}$$
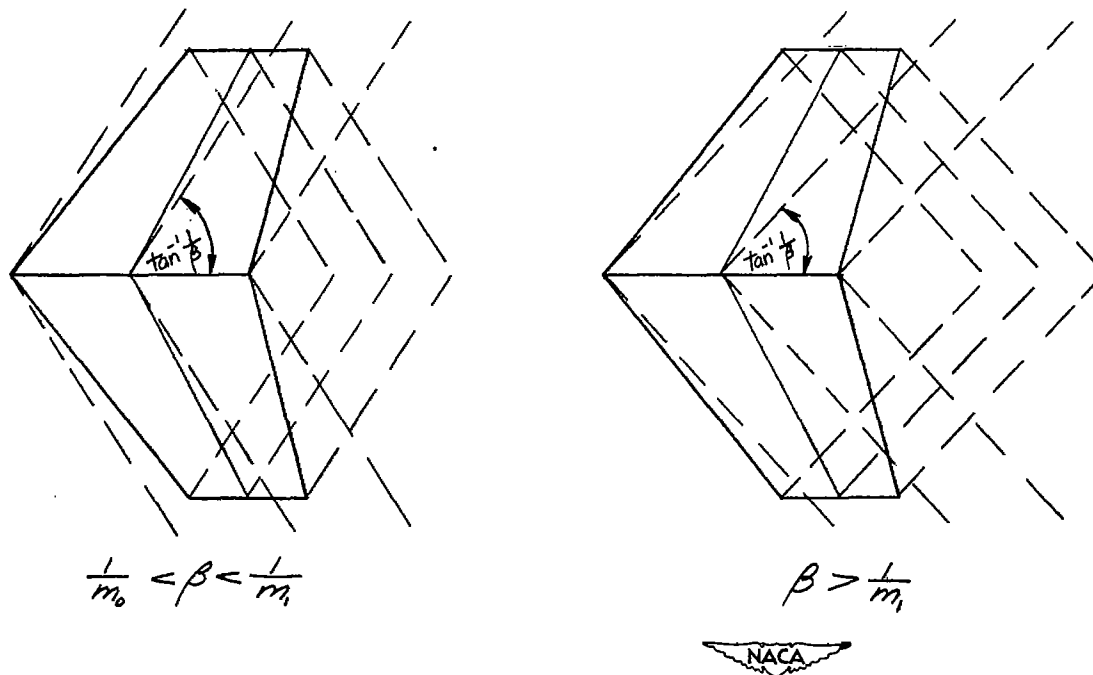
Figure 2.- Mach line configurations for tapered plan forms.

$$\frac{1}{m_0} < \beta < \frac{1}{m_1} \qquad\qquad \beta > \frac{1}{m_1}$$
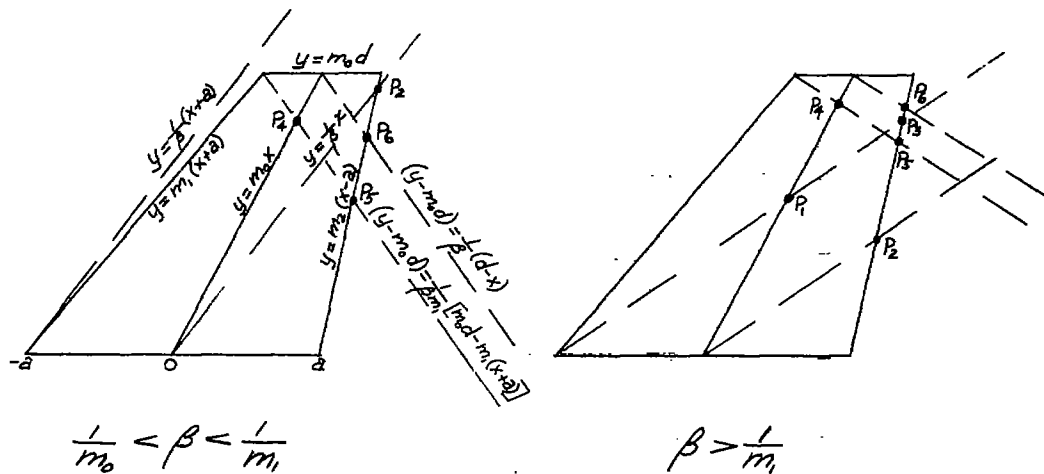
P	y-value	P	y-value
P_1	$\dfrac{am_0}{\beta m_0 - 1}$	P_4	$\dfrac{dm_1{}^2(1+\beta m_1) - am_1 m_0}{m_1(1+\beta m_0)}$
P_2	$\dfrac{am_2}{\beta m_2 - 1}$	P_5	$\dfrac{dm_0 m_2(1+\beta m_1) - 2am_1 m_2}{m_1(1+\beta m_0)}$
P_3	$\dfrac{2am_2}{\beta m_2 - 1}$	P_6	$\dfrac{dm_2(1+\beta m_0) - am_2}{1+\beta m_2}$

Figure 3.- Information pertinent to integration limits in equations (4) and (6).
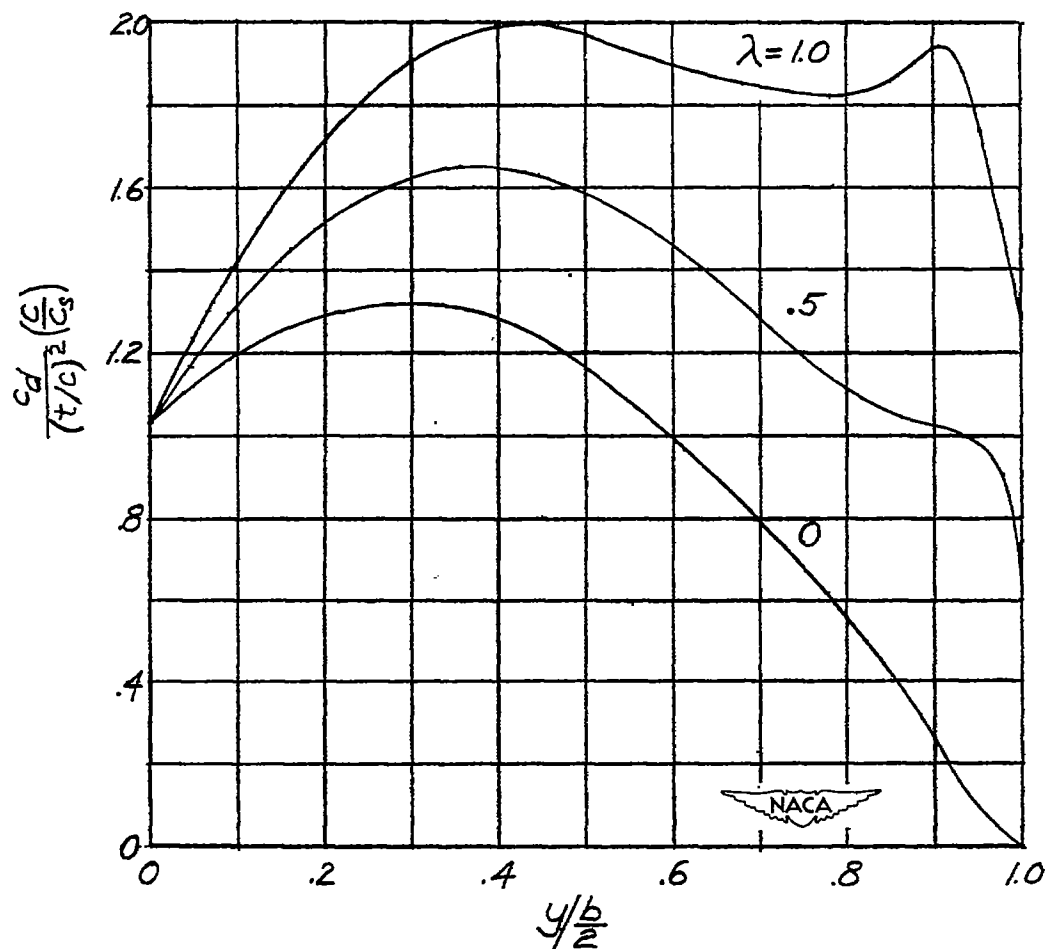
Figure 4.- Distributions of section wave drag for various taper ratios. Aspect ratio, 2; Mach number, 3; sweepback of maximum-thickness line, 60°.
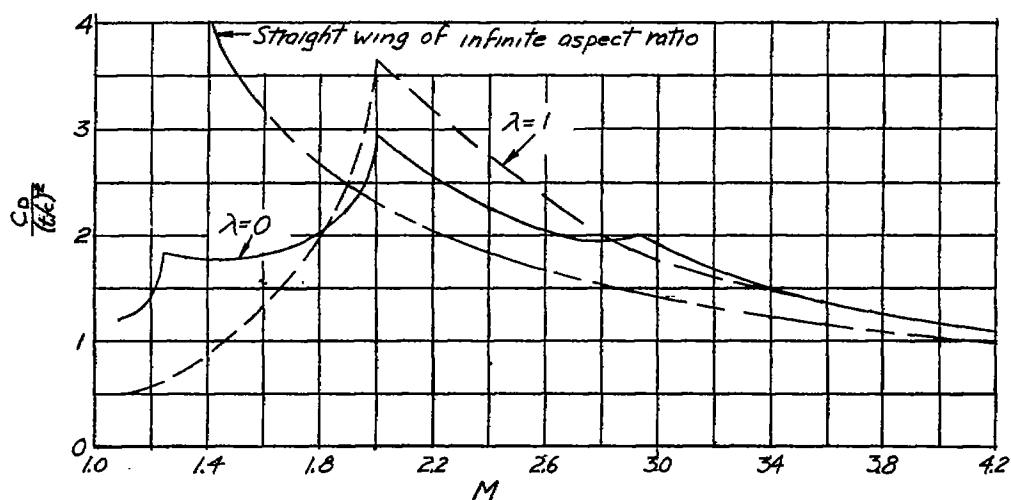
(a) Aspect ratio, 2.
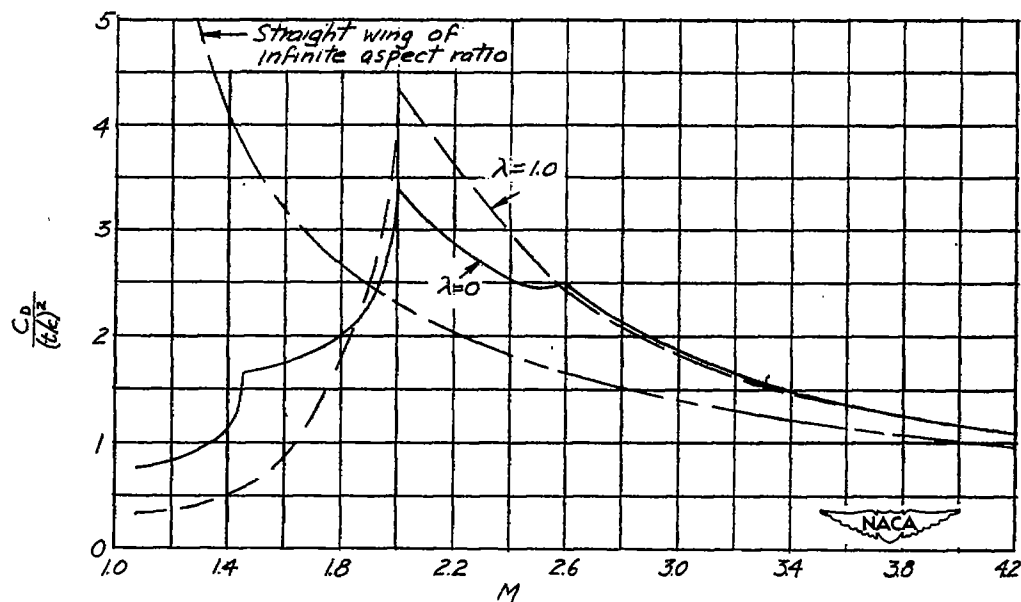
(b) Aspect ratio, 3.

Figure 5.- Variation of wing wave-drag coefficient with Mach number for wings of constant
aspect ratio. Sweepback of maximum-thickness line, 60°. Mach lines are parallel to
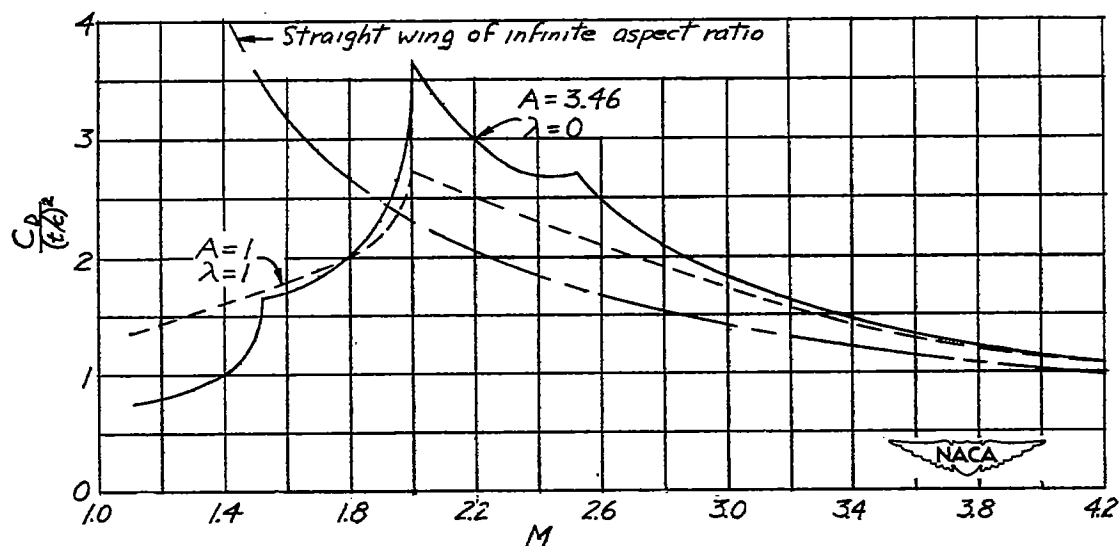the maximum-thickness line at Mach number 2.0.

Figure 6.- Variation of wing wave-drag coefficient with Mach number for wings of equal root
bending stress. Sweepback of maximum-thickness line, 60°. Mach lines are parallel
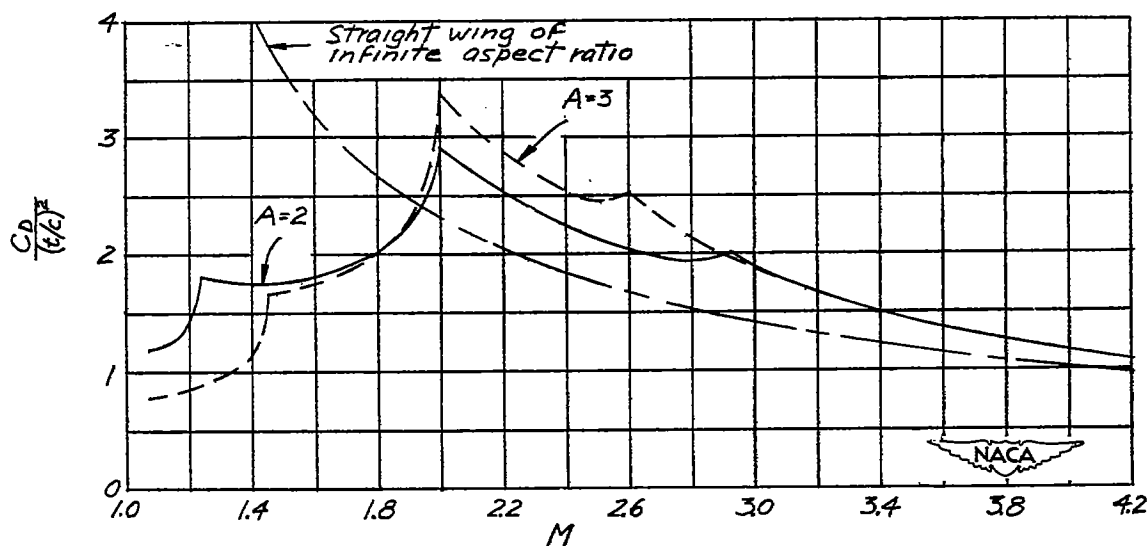to the maximum-thickness line at Mach number 2.0.

Figure 7.- Variation of wing wave-drag coefficient with Mach number for wings of taper ratio 0.
Sweepback of maximum-thickness line, 60°. Mach lines are parallel to the maximum-thickness
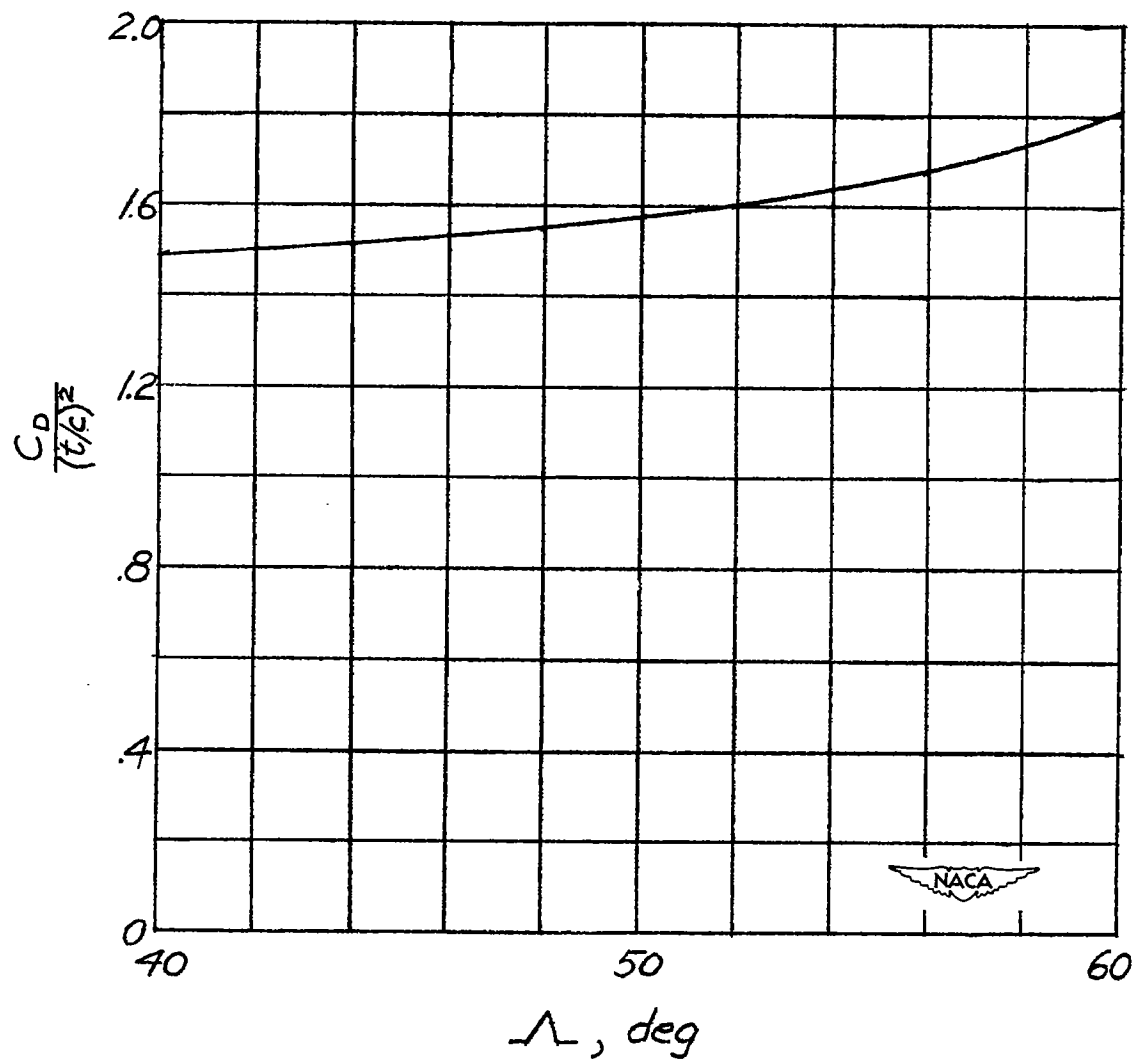line at Mach number 2.0.

Figure 8.- Variation of wing wave-drag coefficient with sweepback of
maximum-thickness line. Taper ratio, 0.5; aspect ratio, 2;
Mach number, 3.